

Structural Peculiarities and Electrophysical Properties of Lithium Ion Conducting Lanthanum Niobate Prepared by Solid-State Reaction and Precipitation from Solution

Anatolii Belous,^{*,[a]} Oksana Gavrilenko,^[a] Olena Pashkova,^[a] Odile Bohnké,^[b] and Claude Bohnké^[b]

Keywords: Niobate / Solid-state reactions / Conducting materials / Sensors

Synthesis of lithium ion conducting niobate was carried out by a conventional solid-state reaction (SSR) and by precipitation from solution (PS). X-ray powder diffraction was used to determine both intermediate phases that are formed during the preparation of these niobate from powder precursors and to determine the structure of sintered ceramics. It is shown that the PS technique leads to the formation of a perovskite phase at a lower temperature relative to the temperature required for the SSR technique. The electrophysical properties of the sintered ceramics were investigated by ac

impedance spectroscopy. It is shown that not only the resistance but also the capacitance of the grain boundary are strongly affected by the method of synthesis used. It was found for the first time that the ceramic obtained from powders prepared by precipitation from solution can be used as pH sensors with good sensitivity (48 mV/pH) in the pH range from 4 to 10 and with a fast response time.

(© Wiley-VCH Verlag GmbH & Co. KGaA, 69451 Weinheim, Germany, 2008)

Introduction

The great interest in complex oxides $\text{La}_{2/3-x}\text{Li}_{3x}\text{V}_{4/3-2x}\text{Nb}_2\text{O}_6$ (where V stands for vacancy) is due to a need for new highly efficient lithium-conducting materials (membranes, electrodes) for various electrochemical devices. These materials have been synthesized for the first time in our group as products of complete aliovalent substitution of La^{3+} and Li^{3+} for Pb^{2+} in the PbNb_2O_6 oxide with a tetragonal tungsten bronze structure.^[1–3] Later on, lithium-containing niobates were synthesized as products of partial aliovalent substitution of Li^+ ions for La^{3+} in the defect perovskite structure $\text{La}_{2/3}\text{V}_{4/3}\text{Nb}_2\text{O}_6$.^[4–6] The fact that $\text{La}_{2/3-x}\text{Li}_{3x}\text{V}_{4/3-2x}\text{Nb}_2\text{O}_6$ have promise in the development of lithium-conducting materials is associated with the peculiarities of the crystal lattice of the lanthanum metaniobate $\text{La}_{2/3}\text{V}_{4/3}\text{Nb}_2\text{O}_6$ with a defect-perovskite structure. The presence of a sufficient number of vacancies and channels within the structure, through which lithium ions move, contributes to fast ion transport in lithium-modified lanthanum niobate.

It is well known that a change in the synthesis conditions of materials affects greatly their electrophysical proper-

ties.^[7,8] Therefore, it was of interest to investigate the effect of the synthesis method on the electrophysical properties of these lithium-containing lanthanum niobates. We focused our attention on two particular methods: the traditional solid-state reaction (SSR) method, which is often used to prepare oxide materials, and the precipitation from solution (PS) method, which has been reported in the literature for the synthesis of various lanthanum niobates.^[9–12] In contrast to the SSR method, the PS method aids the “molecular” homogenization of reagents at an early stage of the precipitation and may lead to grains with particular microstructures and then particular electrophysical properties. The aim of this paper is to present some information about the chemical processes and about the microstructural peculiarities and electrophysical properties, that is, ionic conductivity and pH sensor ability of $\text{La}_{2/3-x}\text{Li}_{3x}\text{V}_{4/3-2x}\text{Nb}_2\text{O}_6$, with $3x = 0.5$, obtained by the PS method. We compared these results with those previously obtained on this particular compound prepared by the SSR method.^[6]

Results and Discussions

Synthesis

Synthesis of these niobates proceeds through the formation of many intermediate phases that have been identified by analysis of the X-ray powder diffraction (XRD) patterns, as shown in Table 1. The mixture of the original reagents in the case of the SSR method consisted, after homogenizing milling and drying, of monoclinic Li_2CO_3 , hexagonal

[a] V.I. Vernadskii Institute of General and Inorganic Chemistry, 32/34 Palladina Avenue, 03680 Kyiv – 142, Ukraine
Fax: +380-44-42-42-211
E-mail: a.belous@list.ru

[b] Laboratoire des Oxydes et Fluorures (UMR6010 CNRS), Institut de Recherche en Ingénierie Moléculaire et Matériaux Fonctionnels (FR 2575 CNRS), Université du Maine, Av. O. Messiaen, 72085 Le Mans, Cedex 9, France

La(OH)₃, and monoclinic Nb₂O₅. The appearance of lanthanum hydroxide and lanthanum oxocarbonate instead of the starting lanthanum oxide is associated with the reaction of H₂O and CO₂ with air. It is observed that the primary phase that appears during synthesis of LLNbO by the SSR method is the phase LiNbO₃ of rhombohedral system. When the temperature is raised above 770 K, a second intermediate phase, LiNb₃O₈ of monoclinic system, appears. As the temperature increases, the LiNb₃O₈/LiNbO₃ ratio decreases. The presence of the phase LiNbO₃ at 1320–1420 K, which is absent in the temperature range 1170–1220 K, indicates that a disproportionation reaction takes place according to Equation (1).



Table 1. Phase composition of the La_{0.5}Li_{0.5}Nb₂O₆ powder prepared by the SSR route and PS route as a function of firing temperature, *T* (the firing time is 1 h). The different phases are given in the order of their decreasing amount.

<i>T</i> [K]	Phase composition	
	LLNbO _{SSR}	LLNbO _{PS}
770	Nb ₂ O ₅ La(OH) ₃ Li ₂ CO ₃ La ₂ O ₂ CO ₃ LiNbO ₃	X-ray amorphous state
870	Nb ₂ O ₅ La(OH) ₃ LiNbO ₃ LiNb ₃ O ₈ La ₂ O ₂ CO ₃	La ₃ NbO ₇ LiNbO ₃
970	LiNb ₃ O ₈ Nb ₂ O ₅ La(OH) ₃ LiNbO ₃	x-phase La ₃ NbO ₇ LiNbO ₃ LiNb ₃ O ₈ LaNbO ₄
1070	–	x-phase La ₃ NbO ₇ LiNb ₃ O ₈ LiNbO ₃ LaNbO ₄ Perovskite
1170	LiNb ₃ O ₈ LaNbO ₄ Nb ₂ O ₅	x-phase LiNb ₃ O ₈ LaNbO ₄ La ₃ NbO ₇ LiNbO ₃ Perovskite
1220	LiNb ₃ O ₈ LaNbO ₄ Perovskite	–
1270	LiNb ₃ O ₈ Perovskite LaNbO ₄	Perovskite LiNbO ₃ LaNbO ₄ Nb ₂ O ₅
1320	Perovskite LiNb ₃ O ₈ LaNbO ₄ LiNbO ₃	Perovskite LaNbO ₄ LiNbO ₃ Nb ₂ O ₅
1420	Perovskite LiNbO ₃ LiNb ₃ O ₈ LaNbO ₄	Perovskite
1470	Perovskite	–

It is obvious from the results of XRD analysis that the formation of the perovskite phase LLNbO_{SSR} occurs at 1220 K. In the temperature range from 1220 to 1420 K, this perovskite formation is accompanied by the consumption of the phases LaNbO₄ and LiNb₃O₈, indicating interaction between them. The formation of a lithium-containing lanthanum niobate, as a single phase, has been established at 1470 K.

Table 1 shows that during the synthesis of LLNbO by the PS method the crystallization of intermediate phases takes place at 870 K. Below 870 K, the powder remains amorphous and then the phase identification is not possible. The temperature at which the defect-perovskite phase LLNbO_{PS} appears is 1070 K, which is 150 K lower than in the case of synthesis of LLNbO_{SSR}. The main difference in the formation of LLNbO_{PS} by precipitation from solution compared to the solid-state reaction method lies in the formation of a large number of intermediate phases when *T* < 1170 K. However, for *T* > 1170 K, the process of formation of the defect-perovskite phase is similar for both synthesis methods (Table 1). The formation of these intermediate phases may play an important role in the microstructure of the prepared powders and therefore on the electrophysical properties of the obtained ceramics.

Microstructural and Structural Peculiarities of LLNbO_{PS}

Figure 1a–c show TEM micrographs of the powders prepared by the PS route and fired at temperatures of 370, 870, 1070 K, respectively, for 1 h. After precipitation and washing and drying at 370 K, the precipitate is formed of very fine particles whose size does not exceed 5 nm (Figure 1a). At 870 K, the crystallization occurs and the intermediate phases can be identified. At the same time grain growth occurs. The powder is made of grains that are around 60 nm in size (Figure 1b). At 1070 K, the perovskite phase appears on the XRD pattern, and the reaction between the precursors has occurred. The average grain size reaches 250 nm (Figure 1c). Figure 1d shows the evolution of the size of the particles as a function of temperature. The evolution of the size of the particles is linear in the temperature range from 800 to 1380 K. At 1380 K, the grain size reaches a value of 450 nm. However, at 1380 K the powder is made not only of the defect-perovskite phase La_{0.5}Li_{0.5}Nb₂O₆ but also of the intermediate phases that did not yet react. To obtain a pure phase of La_{0.5}Li_{0.5}Nb₂O₆ the temperature must be raised up to 1420 K. Figure 2a shows an SEM picture of the surface of a pellet prepared from powder obtained through the PS synthesis route and sintered at 1420 K for 2 h. An average grain size of 2.5 μm is observed. Therefore, the sintering process increases considerably the grain size. For comparison, Figure 2b presents an SEM picture of a pellet obtained from powder synthesized by the SSR method and sintered at 1470 K for 2 h (to obtain a pure perovskite phase according to Table 1). The shape of the grains is different and the latter pellet displays a higher grain size, around 5 μm.

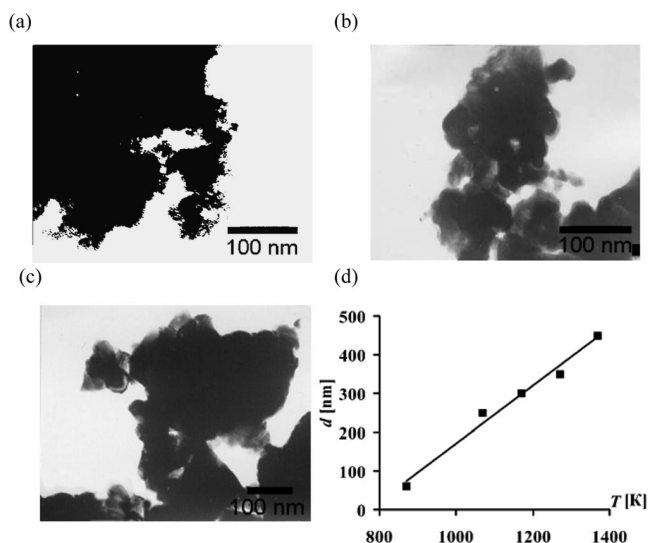


Figure 1. TEM micrographs of the $\text{Li}_{0.5}\text{La}_{0.5}\text{Nb}_2\text{O}_6$ powder prepared by the PS route $[(\text{LLNbO})_{\text{PS}}]$ and fired at different temperatures: (a) 370, (b) 870, (c) 1070 K for 1 h. (d) Particles average size of the $\text{Li}_{0.5}\text{La}_{0.5}\text{Nb}_2\text{O}_6$ powder prepared by the PS route $[(\text{LLNbO})_{\text{PS}}]$ as a function of firing temperatures.

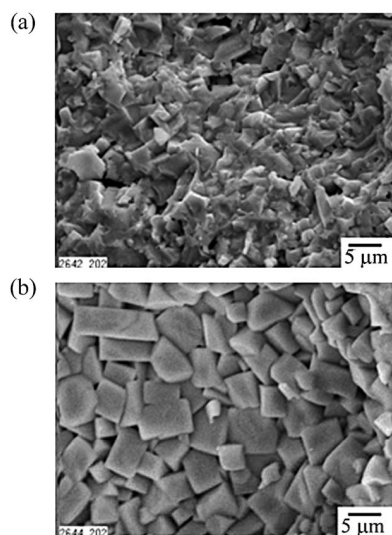


Figure 2. SEM micrographs of a sintered pellet of $\text{La}_{0.5}\text{Li}_{0.5}\text{Nb}_2\text{O}_6$ prepared by the (a) PS route and fired at 1420 K for 2 h and by the (b) SSR route and fired at 1470 K for 2 h.

Figure 3 shows fragments of diffractograms of sintered $\text{LLNbO}_{\text{SSR}}$ and LLNbO_{PS} . The diffractograms show the formation of single-phase products with a defect-perovskite structure with the following lattice parameters: $a = 3.9002 \text{ \AA}$, $b = 3.9005 \text{ \AA}$, $c = 7.8521 \text{ \AA}$ for the SSR sample; $a = 3.9019 \text{ \AA}$, $b = 3.9290 \text{ \AA}$, $c = 7.9149 \text{ \AA}$ for the PS sample. It is obvious from the XRD data that the degree of orthorhombic distortion of the perovskite lattice in the case of the PS method is higher than in the case of the SSR method. This is also indicated by the observed splitting of the (100) and (110) reflection lines for LLNbO_{PS} . The presence of superstructure reflections (001, 101, 111), which indicate La^{3+} ordering in the defect-perovskite structure,^[5,6]

is typical of the diffractograms of both samples. Because of the high temperature used during heat treatment, some Li is lost, as shown by the effects of the synthesis methods on the lithium nonstoichiometry of $\text{La}_{2/3-x}\text{Li}_{3x}\text{V}_{4/3-2x}\text{Nb}_2\text{O}_6$ in ref.^[13] Chemical analysis reveals that an equivalent Li loss of 26 mol-% occurs in $\text{La}_{0.5}\text{Li}_{0.5}\text{Nb}_2\text{O}_6$ ($3x = 0.5$) samples prepared by either the SSR or PS method. Therefore, the degree of orthorhombic distortion cannot be ascribed to different lithium content.

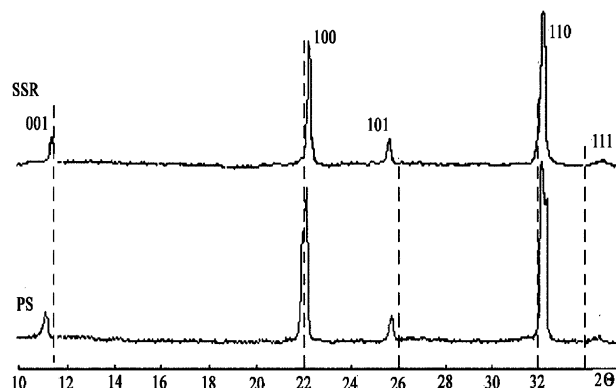


Figure 3. X-ray diffraction patterns of sintered $\text{La}_{0.5}\text{Li}_{0.5}\text{Nb}_2\text{O}_6$ samples prepared by the SSR route and fired at 1470 K for 2 h and by the PS route and fired at 1420 K for 2 h.

Electrophysical Properties of Sintered Niobates

Figure 4a shows typical impedance diagrams (in the Nyquist plane) of lithium-containing lanthanum niobates obtained by the SSR and PS methods. These diagrams have been recorded at 300 K. For ceramic obtained by the SSR the diagram displays a classical shape exhibiting two semicircles and a pike at low frequency. Owing to the value of the capacitances found through the fitting procedure, the high frequency semicircle can be attributed to the motion of the Li^+ ions inside the grains of the ceramic ($C \approx 10^{-11} \text{ F}$) and the second one, at lower frequency, can be attributed to the motion of these ions in the grain boundary ($C \approx 10^{-8} \text{ F}$). The great difference between these capacitances leads to well-separated semicircles. The pike at low frequency with a frequency around μF is attributed to the electrode polarization. The shape of the diagram for the PS sample is totally different exhibiting only one depressed semicircle. This semicircle cannot be fitted with only one relaxation, but instead two are necessary. Such a behavior has already been observed in other oxides prepared by chemistry in solution. This means that in such a case the relaxation due to the ionic motion in the grains and the relaxation due to the ionic motion in the grain boundary have very close time constants. Indeed, fitting results clearly show that the capacitances of bulk and grain boundary are not so different one from the other ($C \approx 10^{-11}$ to 10^{-10} F). The decrease in the grain boundary capacitance is directly linked to the preparation procedure.

Figure 4b presents the value of the total (or effective) conductivity (bulk + grain boundary) of the samples ob-

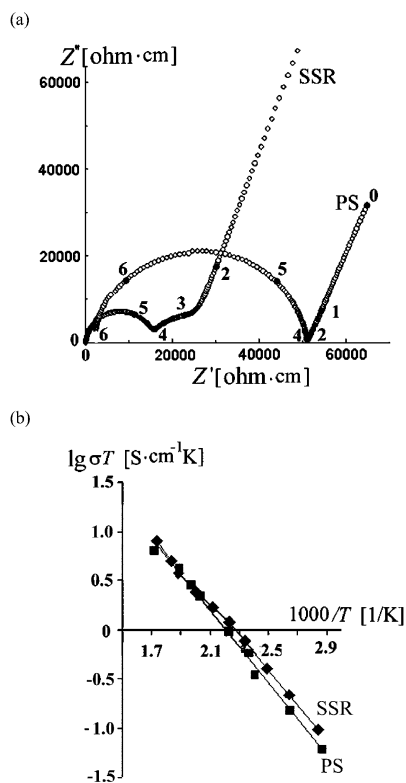


Figure 4. (a) Normalized impedance spectra, recorded at 300 K, of lithium-containing lanthanum niobates prepared by the SSR and by the PS routes. The normalizing factor is the pellet geometric factor. The numbers refer to the frequency power. (b) Arrhenius plots of the total Li-ion conductivity of sintered pellets of $\text{La}_{0.5}\text{-Li}_{0.5}\text{Nb}_2\text{O}_6$ prepared by the SSR and by the PS route.

tained by these two synthesis methods as a function of inverse of temperature. The effective conductivity, at 300 K, is found to be 3.3×10^{-5} and $1.9 \times 10^{-5} \text{ S cm}^{-1}$ for the sample obtained by the SSR and PS routes, respectively. The decrease in the total conductivity of the sample obtained by precipitation from solution is related to an increase in the contribution of the resistance of the grain boundaries.^[14] It is known that the effective resistivity of solid electrolyte increases with decreasing particle size; therefore, we can attribute the small decrease in effective conductivity to the method of synthesis. As shown in Figure 2a, precipitation from solution leads to a finer-grain microstructure. It is worth noting that not only the resistance but also the capacitance of the grain boundary are strongly affected by the method of synthesis used.

The ceramic obtained by the PS method was tested as an ion-selective electrode for pH detection. For this purpose, a highly dense ceramic is necessary. Therefore, the ceramic was sintered at 1420 K for 2 h to improve its compactness (this temperature and time were determined after dilatometry experiments). Figure 5a shows the response of the niobate ceramic as a pH sensor. A linear response is obtained in the pH range from 4 to 10 with a sensitivity of 48 mV/pH unit at 25 °C. As shown in Figure 5b, the response of the sensor to pH variations is fast: only some seconds. The long-term stability of the electromotive force (EMF) re-

mains to be checked. This sub-Nernstian response has been already found with the lithium-containing lanthanum titanates and can be explained by the site-binding model.^[15] This model involves the presence on the oxide surface of basic OH groups that are able to react with protons in solution to charge the oxide surface and to create a potential difference across the ceramic/solution interface. A slightly higher sensibility is found for niobate compared to lithium-containing lanthanum titanates (i.e., 42 mV/pH unit).^[16,17] This difference remains to be explained but it is certainly due to the activity of the basic OH groups. These results show that this niobate is a good candidate for a pH sensor, and it is worth noting that most pH sensor applications (80%) involve the pH range from 4 to 10.

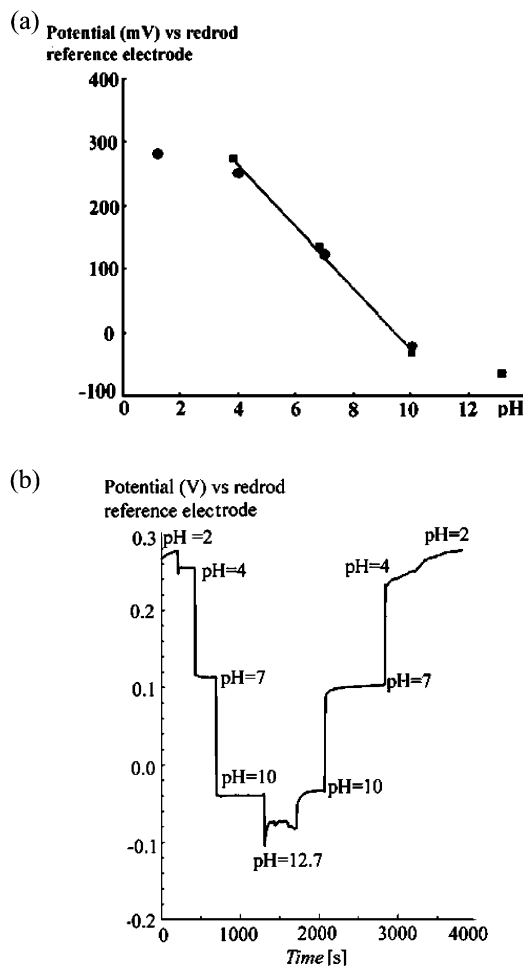


Figure 5. (a) Response of the sintered niobate ceramic as a function of pH. (b) Response of the sintered niobate ceramic as a function of time.

Conclusions

Peculiarities of the structure of lithium-containing lanthanum niobates with defect-perovskite structure by using different synthesis methods have been studied. In the case of the solid-state reaction method, the sequence of reactions during the formation of lithium-containing lanthanum niobate has been determined. It was found that the forma-

tion of lithium-containing lanthanum niobate proceeds by the formation of the intermediate phases LaNbO_4 , LiNbO_3 , and LiNb_3O_8 for $\text{La}_{0.5}\text{Li}_{0.5}\text{Nb}_2\text{O}_6$.

The use of the precipitation from solution method leads to a decrease of 150 K in the temperature of defect-perovskite phase formation and to the formation of finer-grain microstructure in comparison to the solid-state reaction method.

Studies on the electrical properties show that when the synthesis method is used to prepare the niobate powders, the electrical grain boundary resistance and capacitance of the sintered pellets is mostly influenced. This leads to a slight decrease in the effective conductivity of the ceramic relative to that obtained for the sample prepared by precipitation from solution. The sintered ceramic obtained from powders prepared by the PS method is highly dense and can be used as a pH sensor with good sensitivity in the pH range from 4 to 10 and with a fast response time. This result offers a new application for these niobate ceramics.

Experimental Section

The extra-pure oxides La_2O_3 and Nb_2O_5 and the extra-pure carbonate Li_2CO_3 were used as original reagents in the synthesis of $\text{La}_{2/3-x}\text{Li}_{3x}\text{V}_{4/3-2x}\text{Nb}_2\text{O}_6$ ($3x = 0.5$) by the SSR method (named $\text{LLNbO}_{\text{SSR}}$). To remove moisture and adsorbed gases, La_2O_3 , Nb_2O_5 , and Li_2CO_3 were previously heated for 4 h at 1120, 1020, and 570 K, respectively. Owing to the hygroscopic nature of the starting materials, they were weighed immediately after heating and cooling. The mixture was homogenized by milling with a vibrating mill in acetone for 5 h. The predried (370 K) batch was subjected to isothermal heat treatment for 1 h in a temperature range from 770 to 1470 K.

To synthesize $\text{La}_{2/3-x}\text{Li}_{3x}\text{V}_{4/3-2x}\text{Nb}_2\text{O}_6$ ($3x = 0.5$) by the PS method (named LLNbO_{PS}), alcoholic solutions of extra-pure $\text{La}(\text{NO}_3)_3$ and NbCl_5 and aqueous solutions of extra-pure LiOH and NH_4OH were used as original reagents. The NH_4OH solution was added to a mixture of $\text{La}(\text{NO}_3)_3$ and NbCl_5 solutions, taken in a stoichiometric ratio, to pH 9. The obtained precipitate was washed with a 2-propanol/distilled water mixture until free of mother solution. A calculated amount of aqueous LiOH solution was then added to the precipitate whilst stirring and allowed to evaporate at 370 K. The dried powder was subjected to isothermal treatment for 1 h in the temperature range from 770 to 1420 K.

Powders of $\text{La}_{2/3-x}\text{Li}_{3x}\text{V}_{4/3-2x}\text{Nb}_2\text{O}_6$ ($3x = 0.5$) obtained from either the SSR or PS routes were pressed into disks under a pressure of 0.5 MPa and fired at 1320 and 1270 K, respectively (firing time 2 h). The obtained pellets were sintered at 1470 (2 h) and 1420 K (2 h), respectively. The density of the sintered samples ranges from 95 to 98% depending on the sintering temperature.

The phases were identified by X-ray powder diffraction (XRD) recorded at room temperature with a DRON-4-07 diffractometer (Cu-K_α radiation; 40 kV, 18 mA). Data for sintered samples were collected in the 2θ range from 10 to 150° in a step mode with the step $\Delta 2\theta = 0.02^\circ$ and an exposure time of 10 s for each point. SiO_2 (2θ standard) and NIST SRM1976- Al_2O_3 (certified intensity standard) were used as external standards.^[18] The crystal parameters

were refined by using Rietveld full-profile analysis. The microstructural studies of the samples were carried out by using JEM 100 CX and LCXA Syperprobe 7333 electron microscopes.

The electrophysical properties of the ceramic samples were investigated by complex impedance spectroscopy in the frequency range from 1 to 5 MHz by using a 1260 Frequency Response Analyzer and a 1296 Dielectric Interface from Solartron. The measurements were performed in the temperature range from 300 to 600 K under dry N_2 in a two-probe cell (DataLine). It was checked that the electrochemical system remains linear up to 1 V; therefore, the applied ac voltage chosen was 400 mV (r.m.s). Sputtered Pt was used as ion-blocking electrodes.

Sintered and dense ceramics were tested as ion-selective electrodes for pH detection. An Ag/AgCl electrode in contact with a saturated KCl solution, buffered at pH = 7, was used as an internal reference. The external reference was a Red/Rod™ Radiometer electrode. Therefore, the electrochemical cell can be described by the following sequence:

Ag/AgCl/saturated KCl (aq.) pH = 7/ceramic/solution under test/Red/Rod™

The solutions under test were commercial buffered solutions from Radiometer and Carlo Erba. Data were recorded with a Tacussel millivoltmeter (Minisis 8000) and an Agilent 34970A acquisition unit.

- [1] A. Belous, Ye. Novosadova, I. Didukh, Ye. Pashkova, B. Khomenko, *Ionnye Rasplavy i Elektrolity* **1986**, 4, 68–73.
- [2] A. Belous, I. Didukh, Ye. Novosadova, Ye. Pashkova, B. Khomenko, *Neorg. Mater.* **1990**, 26, 1294–1296.
- [3] A. Belous, *Ionics* **1997**, 3, 117–120.
- [4] S. Garsia-Martin, J. Royo, H. Tsukamoto, E. Moran, M. Alario-Franco, *Solid State Ionics* **1999**, 116, 11–18.
- [5] A. Belous, O. Gavrilenko, Ye. Pashkova, V. Mirnyi, *Elektrokhi-miya* **2002**, 38, 479–484.
- [6] A. Belous, Ye. Pashkova, O. Gavrilenko, O. V'yunov, L. Kovalenko, *J. Euro. Ceram. Soc.* **2004**, 27, 1301–1304.
- [7] A. West, *Mir (Moscow)* **1988**, 440 (in Russian).
- [8] I. Wasserman, *Khimiya (Leningrad)* **1980**, 208 (in Russian).
- [9] L. Brixner, J. Whitney, *Mat. Res. Bull.* **1977**, 12, 17–24.
- [10] A. Sych, T. Novik, L. Yeryomenko, *Neorg. Mater.* **1977**, 13, 2046–2051.
- [11] N. Godina, T. Panova, E. Keller, *Neorg. Mater.* **1969**, 5, 1974–1977.
- [12] A. Sych, R. Maksakova, Ye. Kovalenko, *Zh. Neorg. Khim.* **1984**, 29, 1155–1159.
- [13] A. Belous, O. Gavrilenko, E. Pashkova, K. Danil'chenko, O. V'yunov, *Inorg. Mater.* **2004**, 40, 867–873 (translated from *Neorg. Mater.*).
- [14] V. Chebotin, M. Perfilyev, *Khimiya (Moscow)* **1978**, 312 (in Russian).
- [15] R. Van Hal, J. Eijkel, P. Bergveld, *Sens. Actuators, B* **1995**, 24/25, 201.
- [16] C. Bohnke, H. Duroy, J. Fourquet, *Sensors Actuators, B* **2003**, 89, 240.
- [17] M. Vijayakumar, Q. Pham, C. Bohnke, *J. Eur. Ceram. Soc.* **2005**, 25, 2973.
- [18] Certificate of Analysis, Standard Reference Material, **1976**, Instrument Sensitivity Standard for X-ray Powder Diffraction, National Institute of Standards & Technology, Gaithersburg, **1991**, 4.

Received: October 16, 2007

Revised version received: July 15, 2008

Published Online: September 12, 2008